文章编号:1006-9941(2020)02-0127-10

A Mild Method for the Construction of CL-20/H_2O_2 Host-guest Energetic Material

YU Zhi-hui[1], **XU Jin-jiang**[2], **SUN Shan-hu**[2], **WANG Hong-fan**[1], **ZHANG Hao-bin**[2], **DUAN Xiao-chang**[2], **ZHU Chun-hua**[2], **WANG Shu-min**[1], **SUN Jie**[2]

(1. *School of Materials Science and Engineering, Southwest University of Science and Technology, Mianyang* 621010, *China*; 2. *Institute of Chemical Materials, CAEP, Mianyang* 621999, *China*)

Abstract: Hexanitrohexaazaisowurtzitane (CL-20) with a negative oxygen balance, is currently the most powerful commercially available explosive. In this work, the CL-20/H_2O_2 host-guest energetic material (CL-20/H_2O_2) was constructed by using urea hydrogen peroxide (UHP) as raw material through the solvent volatilization at low temperature and negative pressure. The structure of the complex was confirmed through X-ray diffraction (XRD) and Raman spectra. Results indicates that CL-20/H_2O_2 crystallizes in orthorhombic system space group P*bca* with a long-range ordered stacked structure. The ratio of CL-20 molecule and H_2O_2 molecule is 2∶1 stoichiometry according to the thermogravimetry and simultaneous differential scanning calorimetry (TG-DSC) analyses. Furthermore, the polymorph transitions of CL-20/H_2O_2 with increasing temperature were investigated by *in situ* high temperature XRD. Results show that CL-20/H_2O_2 gradually converts to γ-CL-20 with elevated temperature and the rate of transition is faster than that of ε-CL-20. The CL-20 acetonitrile solvate (CL-20/CH_3CN) is a key intermediate *via* a solid state phase transition to form the CL-20/H_2O_2 host-guest energetic material by tracing the growing process of CL-20/H_2O_2.

Key words: host-guest energetic materials; hexanitrohexaazaisowurtzitane (CL-20); H_2O_2; metastable phase; solid state transition phase

CLC number: TJ55; O62 **Document code**: A **DOI**: 10.11943/CJEM2019064

1 Introduction

Energetic materials are extensively used for a variety of military purposes, industrial applications and aerospace fields.High energy density materials (HEDMs) with desired properties are already attracting wide attention in recent decades[1-4]. The performance of HEDMs is dominated by detonation pressure(p) and velocity(D), which are connected with density and oxygen balance (OB)[5-6]. Recent concerns about the level of environmental compatibility of energetic materials have been focused on the green energetic materials based on a good OB[7-8]. Many attributions were made to tune these materials through the physical and chemical approaches. In general, load oxidizer such as ammonium nitrate (AN), hydrazine nitroform (HNF), ammonium dinitramide (ADN) and ammonium perchlorate (AP) in energetic materials to enhance the explosive performance. However, this method would decrease the loading of explosives. Therefore, another way is to design and synthesize novel energetic compounds with a good OB, typical nitrogen-rich heterocycles such as tetrazole, triazole, furazan, and tetrazine derivatives[9-10].However, the exploitation of novel energetic materials is a long-term challenge with remarkable obstacle. Current interest has been focused on the development of host guest energetic materials, such as hexanitrohexaazaisowurtzitane (CL-20)/N_2O

Received Date: 2019-03-16; **Revised Date**: 2019-24-26

Published Online: 2019-09-02

Project Supported: National Natural Science Foundation of China (21805259).

Biography: YU Zhi-hui (1993-), female, master student, crystal engineering of energetic materials. e-mail: s3071098@163.com

Corresponding author: WANG Shu-min (1974-), male, professor, modification of crystal. e-mail: shu_minwang@163.com.

Sun Jie (1972-), male, professor, crystal engineering of energetic materials. e-mail: sunjie@caep.cn

引用本文:余治慧,徐金江,孙善虎,等. 晶胞内嵌H_2O_2分子的CL-20基主客体炸药的温和制备[J]. 含能材料,2020,28(2):127-136.

YU Zhi-hui, XU Jin-jiang, SUN Shan-hu, et al. A Mild Method for the Construction of CL-20/H_2O_2 Host-guest Energetic Material[J]. *Chinese Journal of Energetic Materials (Hanneng Cailiao)*, 2020, 28(2):127-136.

host-guest energetic material and CL-20/H_2O_2 host-guest energetic material(CL-20/H_2O_2), which can improve the explosive performance significantly[11-12].

As is well known, CL-20 has been widely studied as one of the most powerful commercially available explosives. Given an insight into the lattice packing model of CL-20, the instinct cavities can be used to insert the specific small molecules, such as H_2O, CO_2 and N_2O[11-13]. As a result, the CL-20/H_2O_2 attracted our attentions. Matzger incorporated H_2O_2 into CL-20 crystal by solvent crystallization, which improved the OB and the crystal density. However, the high concentration H_2O_2 (98%) was used as a solvent, which was a extremely dangerous method. Therefore this synthesis route appeared to be difficult in a large number production of CL-20/H_2O_2. Therefore, it is urgent to develop a convenient and safe method to prepare CL-20/H_2O_2.

In this study, a safe and mild method was developed to prepare the CL-20/H_2O_2. Especially, urea hydrogen peroxide (UHP) is adopted to replace concentrated H_2O_2. The structure determination, morphology characterization, thermal behaviour, sensitivity and phase transition of this complex were carried out. Furthermore, the mechanism was examined by PXRD and Raman spectra in detail. This study provides an effective method which encapsulating the specific molecules in the lattice cavity to design high-performance energetic materials.

2 Experimental

2.1 Materials

Raw CL-20 was provided by the Institute of Chemical Materials, Chinese Academy of Engineering Physic (CAEP). Acetonitrile (CH_3CN, 99.9%, Superdry, dried in the 4Å molecular sieve), was provided by J&K Chemical Reagent Factory. Anhydrous ether (99.5%) was purchased from Chengdu Kelong Chemical Reagent Factory. Urea Hydrogen peroxide (UHP, 97%) and molecular sieve were purchased from Aladdin industrial corporation Chemical Reagent Factory.

2.2 Preparation of CL-20/H_2O_2

According to the properties of H_2O_2, ether was applied to extract hydrogen peroxide from UHP at low temperature, since it had a high solubility for hydrogen peroxide but not for urea and low boiling point which is easy to volatile. In addition, in this work, it was a good selection to adsorb the solution by molecular sieve. CL-20/H_2O_2 was obtained until the solvent disappeared and there were no by-products.

The preparation of CL-20/H_2O_2 was carried out at 0-5 ℃. As shown in Fig.1a, UHP (5 g) was added into anhydrous ether (20 mL) and exhaustively stirred for 3 h at 0 ℃. Then H_2O_2 was extract by filter

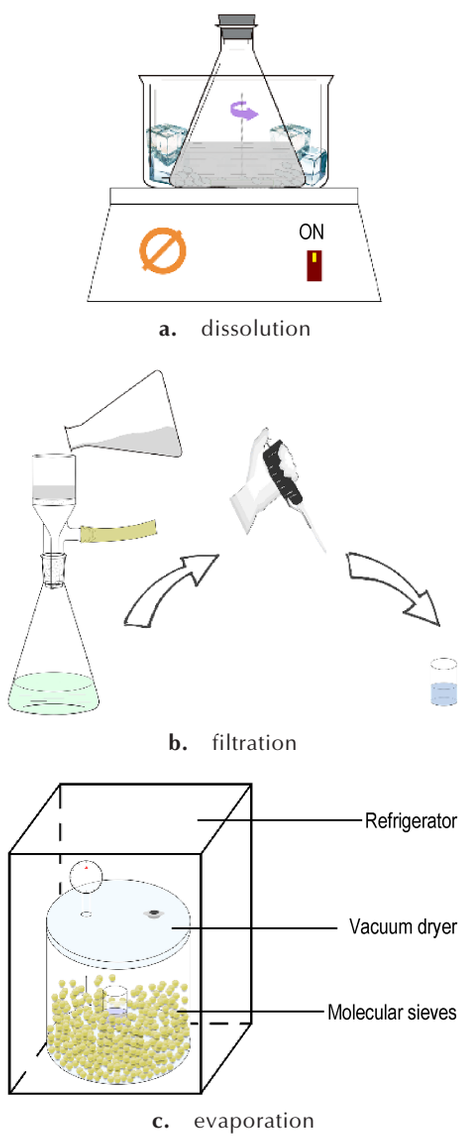

a. dissolution

b. filtration

c. evaporation

Fig. 1 The preparation sketch of CL-20/H_2O_2

operation, as depicted in Fig.1b, 10 mL H_2O_2 extract was injected to a glass vial which was loaded with the solution of ε-CL-20 (0.2 g) in dry acetonitrile (1 mL). As seen in Fig.1c, the vial was put into a vacuum dryer with molecular sieves at 0−4 ℃ and −0.06 − −0.05 MPa. CL-20/H_2O_2 was obtained until the solution evaporated completely.

2.3 Mechanism Experiment of Solid-state Phase Transition

To verify the formation of CL-20/H_2O_2 via a solid-state phase transition, mechanism experiments were carried out.

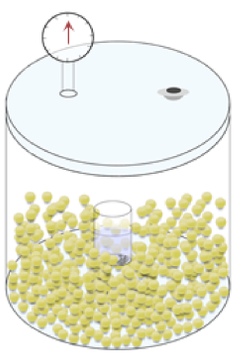

a. experiment A

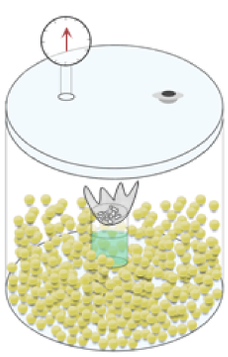

b. experiment B

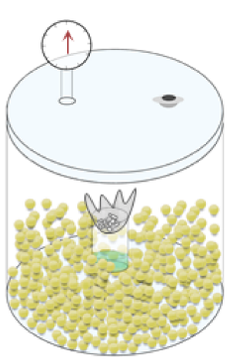

c. experiment C

Fig. 2 Mechanism experiments of CL-20/H_2O_2 solid-state phase transition

Experiment A: As shown in Fig.2a, 0.3 g ε-CL-20 was dissolved into 600 μL acetonitrile and the solution was added into vial, then 10 mL H_2O_2 was loaded into the vial. The vial was put into a vacuum dryer with molecular sieves to volatilize (the temperature of the vacuum dryer was remained at 0−4 ℃ and the pressure of the vacuum was kept at −0.06 − −0.05 MPa).

Experiment B: As shown in Fig.2b, 0.3 g CL-20/CH_3CN was loaded in dense gauze and was suspended in the mouth of vial. And 10 mL H_2O_2 extract was loaded in vial, then the vial was put in a vacuum dryer in the same condition as experiment A.

Experiment C: As shown in Fig.2c, a vial loaded with 10 ml H_2O_2 extract was placed into a vacuum dryer to volatilize at 0−4 ℃ and −0.05− −0.06 MPa. When H_2O_2 extract was less than half in vial, the vial was taken out, 0.3 g CL-20/CH_3CN was placed in a dense gauze and suspended into the mouth, and then put back. Keep evaporating until the disappearance of the solution.

2.4 Characterizations

PXRD were recorded on a Bruker D8 Advance X-ray diffractometer equipped with Cu K_α radiation source (40 kV, 40 mA). Raman were conducted on a Renishaw (UK, model InVia) with the 532 nm laser excitation. The thermal behavior was investigated at 25− 300 ℃ through the TG-DSC, the sample was heated with a heating rate of 10 ℃·min^{-1} under the nitrogen flow. Microstructures of CL-20/H_2O_2 were collected on a scanning electron microscope on an Apollo 300 operating at an acceleration of 3 kV. The crystal morphologies were observed via ZEISS 2000-C optical microscope in reflection mode. The polymorph transitions were analyzed by *in situ* high temperature XRD with a temperature programming. The scanning data were collected during temperature from 30− 185 ℃ in an interval of 5 ℃ at a fixed heating rate of 5 ℃·min^{-1}. At last, the temperature was reduced to 30 ℃ and the final scanning process was carried out. Moreover, the polymorphic con-

tents of γ-CL-20 were quantified by Topas software[15]. The impact sensitivity was according to the GJB772A−1997 standard method 601.2. Conducted by small-scale impact drop testing with a 2 kg drop mass on approximately 30 mg samples, which was determined statistically with the drop height of 50% explosion probability (H_{50}). The friction sensitivity was determined with a WM-1 type friction sensitivity instrument according to GJB-772A−1997 standard method 602.1. Measured with 1.5 kg pendulum mass on 20 mg sample. For comparison, the sensitivity of raw material ε-CL-20 was also tested.

3 Results and Discussion

3.1 Crystallization of CL-20/H_2O_2

The PXRD pattern of the experimental CL-20/H_2O_2 is shown in Fig. 3a, which mathches with the simulated pattern of CL-20/H_2O_2 (CCDC: 1495520). Additionally, the experimental data of CL-20/H_2O_2 are in accordance with those of α-CL-20 (CCDC: 1495519) which indicate that experimental sample of CL-20/H_2O_2 and α-CL-20 have the same space group of P*bca* and exhibit in a rhombic packing[11]. Moreover, Raman spectra of the CL-20/H_2O_2, α-CL-20 and raw materials (UHP and ε-CL-20) are displayed in Fig.3b and Fig.3c. The spectrum of the experimental CL-20/H_2O_2 is similar to that of α-CL-20 and is different from that of ε-CL-20. The strong peak of experimental CL-20/H_2O_2 at 3557 cm^{-1} could be attributed to the stretching vibration of O—H bond assigned to H_2O_2. In contrast with α-CL-20, O—H vibration at 3610 cm^{-1} is assigned to H_2O. Moreover, the characteristic peak of O—O bond stretching vibration for sample could be seen at 866 cm^{-1} in the experimental CL-20/H_2O_2. Compared with that of UHP (located at 871 cm^{-1}), the peak decreases approximately at 866 cm^{-1}, which is caused by the hydrogen bond between H_2O_2 and CL-20. The results of Raman spectra are in good agreement with that of CL-20/H_2O_2 in reference[11].

The thermal behavior of experimental CL-20/H_2O_2 and raw material ε-CL-20 are shown in Fig.4a

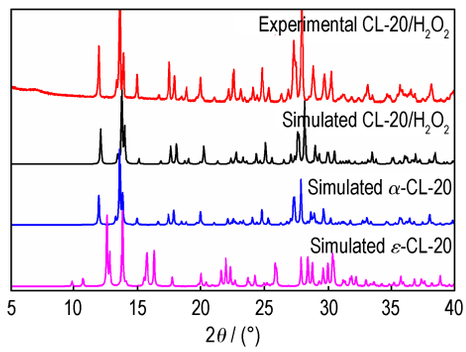

a. PXRD patterns

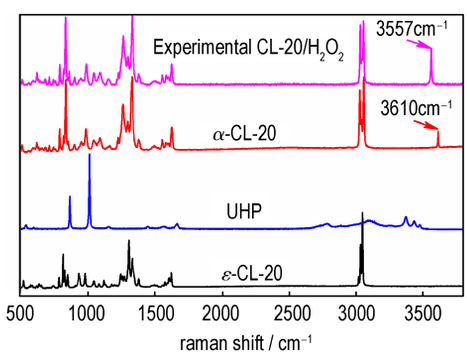

b. Raman spectra

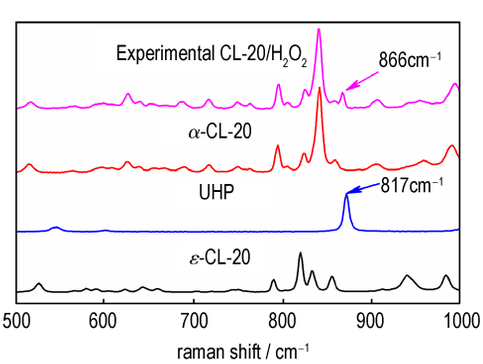

c. zoomed in (500 − 1000 cm^{-1}) Raman spectra

Fig. 3 Identification of obtained CL-20/H_2O_2

and Fig.4b. Compared to ε-CL-20, the TG analysis of experimental CL-20/H_2O_2 shows a remarkable mass loss about 3.4% at 160−167.3 ℃. Corresponding to the DSC profile, there are two exothermic peaks (162.5, 252.0 ℃) and a sharp endothermic peak at 167.3 ℃ for CL-20/H_2O_2. In contrast with ε-CL-20, there is no mass loss before 200 ℃ in TG curve, and its DSC profile displays an endothermic peak at 166.9 ℃ and one exothermic peak at 238.7 ℃[16]. The mass loss is confirmed to be H_2O_2 and the stoichiometric ratio of CL-20 to H_2O_2 is 2∶1 (calculated value: 3.7%). The H_2O_2 molecules embedded in

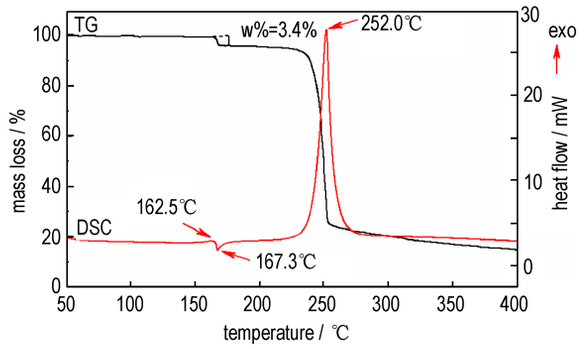

a. CL-20/H_2O_2

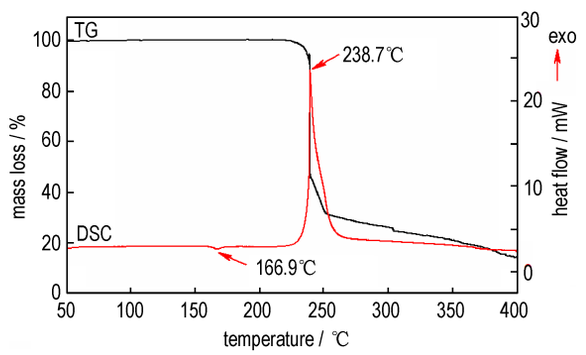

b. ε-CL-20

Fig. 4 TG-DSC curves of CL-20/H_2O_2 and ε-CL-20.

voids of CL-20 crystal lattice firstly decomposes at 165 ℃, followed by a phase transition to the γ-CL-20 at 167.3 ℃ (supported by *in situ* PXRD below). H_2O_2 is unstable and easily broken down in the air. However, the embedding of H_2O_2 into the capsule-shaped voids of CL-20 could delay the decomposition, in other words, the H_2O_2 in the voids is more stable than that in air. Additionally, the structure stability and the decomposition temperature of CL-20/H_2O_2 are higher than ε-CL-20, due to the incorporation of guest molecule and the change of lattice packing.

The SEM images of CL-20/H_2O_2 are showed in Fig.5, which revealed the three-dimensional porous distribution on the surface and the inner of experimental CL-20/H_2O_2 randomly. This may result from the embedding of H_2O_2 molecule. In addition, there are some cracks on the surface of the sample. The thermal phenomenon of CL-20/H_2O_2 have a higher decomposition temperature which may be related to its porous microstructure of CL-20/H_2O_2. In addition, the appearance of small inhomogeneous holes and cracks may be due to its growth mechanism.

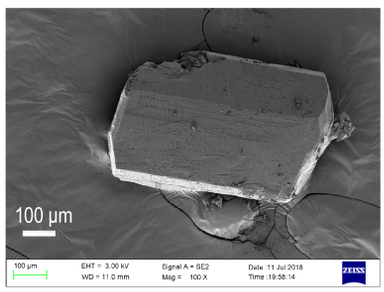

a. integral

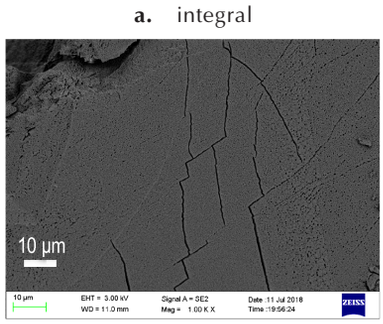

b. surface

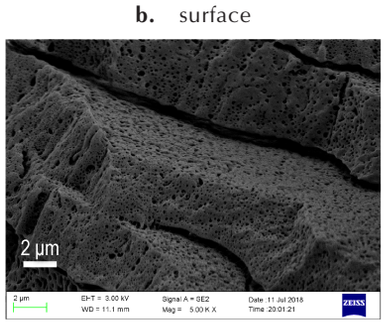

c. cross-section

Fig. 5 SEM images of CL-20/H_2O_2

Table 1 shows the impact and friction sensitivity of ε-CL-20 and CL-20/H_2O_2. The 50% impact height (H_{50}) of CL-20/H_2O_2 is 13.8 cm, close to the raw material ε-CL-20 with 14 cm. The friction sensitivity of CL-20/H_2O_2 is consistent with that of ε-CL-20 which all 100% ignited. The results reveal that CL-20/H_2O_2 and ε-CL-20 exhibited similar sensitivity.

Table 1 Sensitivity of ε-CL-20 and CL-20/H_2O_2

sample	H_{50} / cm	friction sensitivity / %
ε-CL-20	14	100
CL-20/H_2O_2	13.8	100

Note: H_{50} represents the height from which the impact has 50% probability of causing detonation.

3.2 Phase Transformations of CL-20/H_2O_2 with Elevated Temperature

The phase transitions of CL-20/H_2O_2 with increasing temperature were investigated by *in situ* high temperature XRD and the results are presented in Fig.6a. From ambient temperature to 140 ℃, the results of PXRD of CL-20/H_2O_2 agree well with the simulated results of CL-20/H_2O_2[11]. When the temperature is up to 155 ℃, the intensity of the weak peaks at 12.8° (triplet) and 15.5° increases. With the increase of temperature, the intensity of 12.8° (triplet) and 15.5° becomes stronger which is attributed to the emergence of the γ-CL-20 phase gradually. In addition, the characteristic peaks of CL-20/H_2O_2 (12°,15.1°,17.9° and 18.8°) become weak and disappear. And the rate of transition becomes large during 155−165 ℃. Until to 185 ℃, CL-20/H_2O_2 pattern is in accordance with the simulated pattern of γ-CL-20 completely. For ε-CL-20, the result is identical to the previous work (Fig.6b)[15]. The phase contents of γ-CL-20 of CL-20/H_2O_2 and ε-CL-20 with elevated temperature are depicted in Fig. 6c. Compared to ε-CL-20, CL-20/H_2O_2 has a higher phase transition temperature, indicating that CL-20/H_2O_2 is more stable than ε-CL-20. Furthermore, it would entirely transform into γ-CL-20 at 185 ℃, because the H_2O_2 resolves into O_2 and H_2O when temperature is over 140 ℃, and produce interspace in the crystal structure to make the transition easier.[12,17]

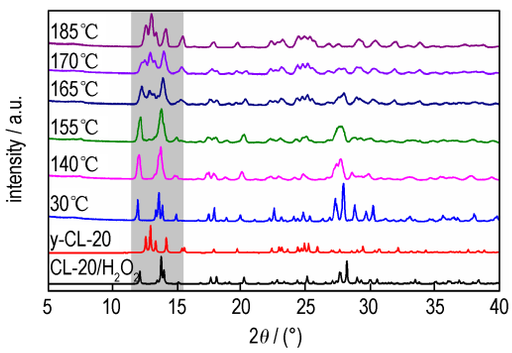

a. *in situ* PXRD patterns of experimental CL-20/H_2O_2

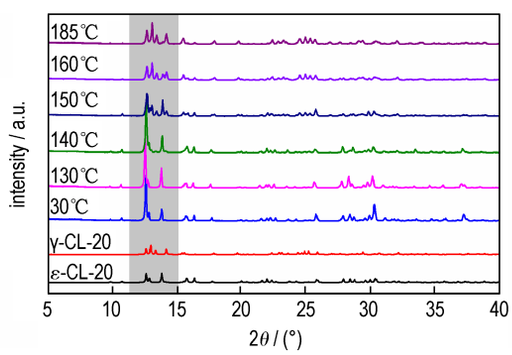

b. *in situ* PXRD patterns of ε-CL-20

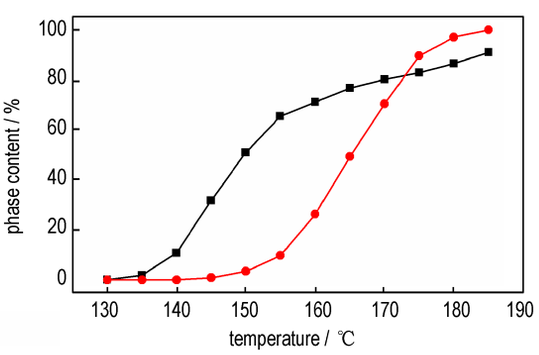

c. evolution of phase transition of experimental CL-20/H_2O_2 and ε-CL-20 at elevated temperature

Fig. 6 Polymorph transitions of experimental CL-20/H_2O_2 and ε-CL-20 at elevated temperature.

3.3 Insight Mechanism of CL-20/H_2O_2 Formation

In order to make the formation of the CL-20/H_2O_2 energetic material clear, Raman spectra were utilized to analysis the crystallization process of samples. Crystallization process can be divided into 3 stages. When the H_2O_2 extract was added into the CL-20 acetonitrile solution, crystal precipitated from the solvent, and its spectrum is shown in Fig.7a. In comparison with the literature[18], the crystal is found to be CL-20/CH_3CN and this process is defined to be stage 1. The crystal was exposed to gaseous environment gradually as solvent volatilize. The spectral analysis indicates that the composition of the solid phases starts to change and the critical state is called state 2. Peak at 2255 cm^{-1} dominated by CL-20/CH_3CN became weaker, simultaneously, two characteristic peaks at 866 cm^{-1} and 3557 cm^{-1} appeared which was attributed to the formation of CL-20/H_2O_2[11]. This indicates that the stage 2 is the state in which CL-20/CH_3CN gradually transformed to CL-20/H_2O_2. With the disappearance of solvent, stage 3 emerges, the spectral analysis shows that the characteristic peak at 2245 cm^{-1} of CL-20/CH_3CN has disappeared totally, peaks at 866 cm^{-1} and 3557 cm^{-1} ascribed

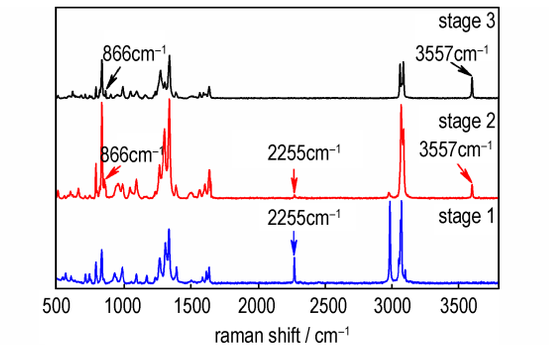

a. Raman spectra of samples from crystallization process

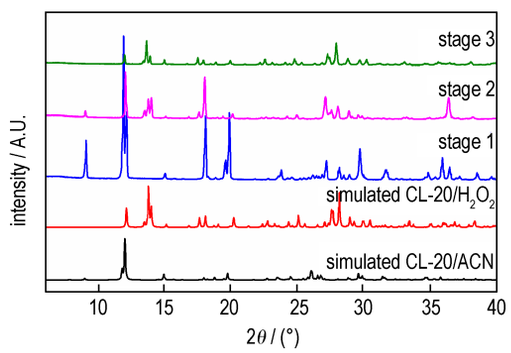

b. PXRD patterns of samples from crystallization process

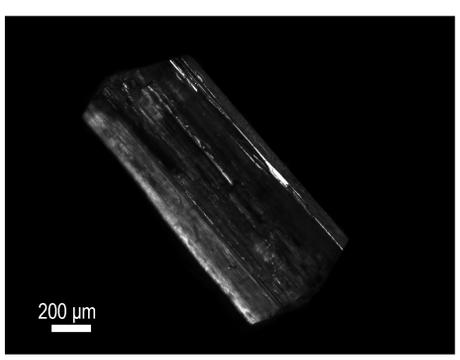

c. morphology of CL-20/CH_3CN

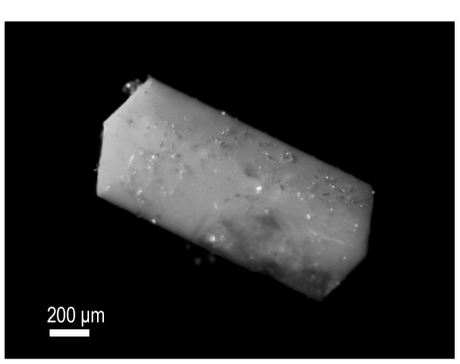

d. morphology of CL-20/H_2O_2

Fig. 7 The formation process of CL-20/H_2O_2

to CL-20/H_2O_2 has developed further. These changes suggest that the complete emergence of CL-20/H_2O_2.

PXRD was employed to detect the formation process accurately. As seen in Fig. 7b, the results show a good agreement between the PXRD pattern of the samples from solvent (stage 1) and the simulated CL-20/CH_3CN (CCDC: 1569059). Once the crystal exposed to gas environment (stage 2), the PXRD pattern begins to change. Diffraction peak at 8.94° of CL-20/CH_3CN becomes increasingly weaker as the solvent volatilizes, and the diffraction peaks referred to CL-20/H_2O_2 (a triplet around 13.7° and a peak of 17.62°) can be observed clearly. As the disappearance of the solvent (stage 3), diffraction peaks of CL-20/H_2O_2 can be observed merely[18]. The changes of PXRD are in accordance with Raman results, revealing that the CL-20/CH_3CN is a key intermediate for the formation of CL-20/H_2O_2.

Along with morphological change of the sample in preparation process, CL-20/CH_3CN as an intermediate and preparation process can be concluded as a solid-state phase transition. The image of sample at the end of stage 1 is shown in Fig.7c. It is a transparent sample with a colourless cubic crystal. By contrast, the crystal from stage 3 (Fig.7d) retained original shape, however, it becomes an opaque crystal[19]. It can be implied that the CL-20/H_2O_2 is obtained based on CL-20/CH_3CN without the dissolution-recrystallization process.

To explore mechanism further, the crystal structure of CL-20/CH_3CN and CL-20/H_2O_2 were investigated (Fig. 8). The formation of CL-20/CH_3CN depends on hydrogen bonds between CL-20 molecules and acetonitrile molecules, with intermolecular distances of 2.362 Å, 2.573 Å and 2.411 Å, respectively. For CL-20/H_2O_2, the H_2O_2 molecule interaction with two CL-20 molecules are via hydrogen bonds, with bond lengths of 2.224, 2.294, 2.224 Å and 2.259 Å, respectively. Manifestly, each hydrogen bond in CL-20/H_2O_2 is stronger than that of CL-20/CH_3CN. Therefore, the transformation from CL-20/CH_3CN (metastable phase) to CL-20/H_2O_2 (stable phase) is a spontaneous process thermodynamically[20]. It was a convincing evidence that the formation of CL-20/H_2O_2 via an intermediate of CL-20/CH_3CN.

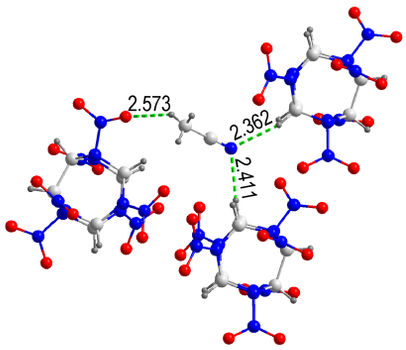

a. hydrogen bonding interaction between CL-20 and CH_3CN

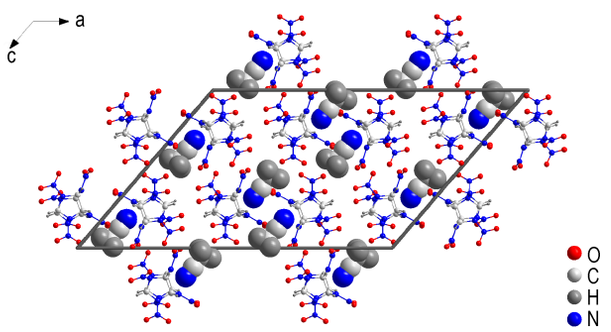

b. crystal packing diagram in the unit cell of CL-20/CH_3CN along the b-axis

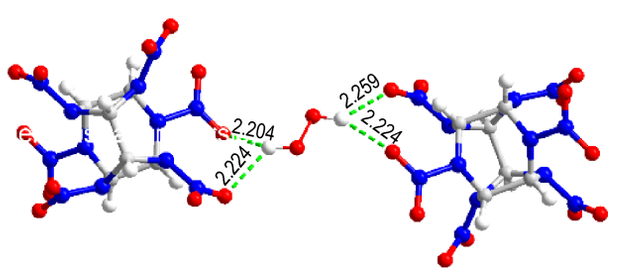

c. hydrogen bonding interaction between CL-20 and H_2O_2

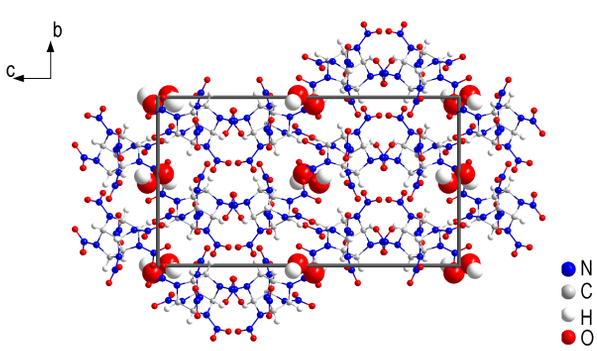

d. crystal packing diagram in the unit cell of CL-20/H_2O_2 along the a-axis

Fig. 8 Hydrogen bonding and crystal packing diagrams of CL-20/H_2O_2 and CL-20/CH_3CN

The morphology change has implied that there is a solid-state phase transition between the CL-20/H_2O_2 and CL-20/CH_3CN. To make the transformation process clearer, the mechanism experiments were carried out. The samples from experiment A, B and C were tested by PXRD and Raman spectra. As shown in Fig.9a, the PXRD patterns of the samples of experiment A and C were assigned to CL-20/H_2O_2. However, the peaks of sample in experiment B can be well identified to β-CL-20. The results of mechanism experiments were further confirmed by Raman spectra shown in Fig. 9b. In experiment A, CL-20/CH_3CN was soaked in solution, as the ether evaporated, phase transition occurred until it is exposed to the concentrated H_2O_2 gas molecules. In experiment B, however, when the CL-20/CH_3CN was suspended in vial, the gas molecules were almost ether vapor, few H_2O_2 molecules exist. And in experiment C, CL-20/CH_3CN was surrounded by the gas molecules H_2O_2 and ether. Therefore, it can be concluded that the preparation of CL-20/H_2O_2 is a solid-state phase transition process which is induced by H_2O_2 gas molecules.

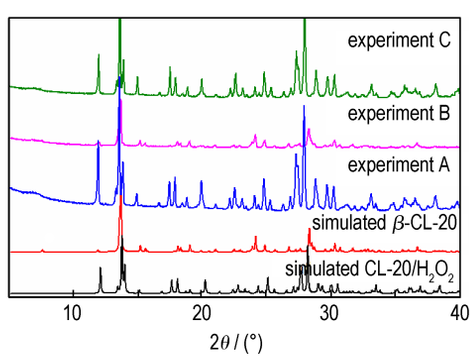

a. PXRD patterns

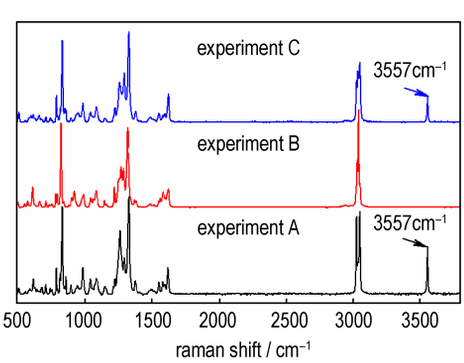

b. Raman spectra

Fig. 9 PXRD patterns and Raman spectra of mechanism experiments A, B and C

4 Conclusions

A mild method is utilized to prepare CL-20/H_2O_2 by evaporation of the solution contained H_2O_2 and CL-20 without by-product. It is found that CL-20/H_2O_2 would have cause a mass loss about 3.4% around 162.5 ℃ caused by the deformation of H_2O_2, and the phase transitions was detected with *in situ* high temperature XRD. It is found that the CL-20/H_2O_2 was stable up to 140 ℃, then converted to γ-CL-20 quickly during the temperature range of 140-170 ℃. And the SEM show that CL-20/H_2O_2 by this method would have a three-dimensional porous structure, and it may lead to a similar impact sensitivity and friction sensitivity to ε-CL-20. Moreover, a convincing evidence given by PXRD patterns, Raman spectra and optical images pointed out that the formation of CL-20/H_2O_2 via a metastable phase CL-20/CH_3CN solvate. The conditions of the phase transition was studied by the mechanism experiments, which reveal that CL-20/CH_3CN transformed into CL−20/H_2O_2 is a process induced by the H_2O_2 molecules. The simple preparation strategy of CL-20/H_2O_2 host-guest energetic material makes it possible for a large-scale production. Furthermore, the preparation method of stable phase via a metastable phase can be a promising approach to construct a novel energetic materials.

References:

[1] Zhang J, Hou T, Zhang L, et al. 2,4,4,6,8,8-Hexanitro-2,6-diazaadamantane: A high-energy density compound with figh stability[J]. *Organic Letter*, 2018, 20(22): 7172−7176.

[2] Wang Y, Liu Y, Song S, et al. Accelerating the discovery of insensitive high-energy-density materials by a materials genome approach[J]. *Nature Communication*, 2018, 9(1), 2444: 1−11.

[3] Zhang W, Zhang J, Deng M, et al. A promising high-energy-density material[J]. *Nature Communication*, 2017, 8(1), 181: 1−7.

[4] Huang H, Huang H. Insights into the development for post-CHNO energetic materials[J]. *Materials China*, 2018, 37(11): 889−895.

[5] Tang Y, Srinivas D, Grogroy H I, et al. Nitramino-and dinitromethyl−substituted 1,2,4-triazole derivatives as high-performance energetic materials[J]. *Chemistry-A European Journal*, 2017, 23(38): 9185−9191.

[6] Huang C, Xu J, Tian X, et al. High-yielding and continuous fabrication of nanosized CL-20-based energetic cocrystals via electrospraying deposition[J]. *Crystal Growth & Design*, 2018, 18(4): 2121−2128.

[7] Kukuljan L, Kranjc K. 3-(5-amino-1,2,4-triazole)-1,2,4-oxadiazole: A new biheterocyclic scaffold for the synthesis of energetic materials[J]. *Tetrahedron Letters*, 2019, 60(2): 207−209.

[8] Sabrina H, Djalal T, Slimane A, et al. 5-nitro-1,2,4-triazole-3-one: a review of recent advances[J]. *Chinese Journal of energetic materials* (*Hanneng Cailiao*). 2019, 27(4): 326−347.

[9] Kettner M A, Klapotke T M. 5,5'-Bis-(trinitromethyl)-3,3'-bi-(1,2,4-oxadiazole): a stable ternary CNO-compound with high density[J]. *Chemical Communications*, 2014, 50(18): 2268−2270.

[10] Wang G, Lu T, Fan G, et al. Synthesis and properties of insensitive [1-2,4] triazolo [4,3-b]-1,2,4,5-tetrazine explosives[J]. *New Journal of Chemistry*, 2019, 43(4): 1663−1666.

[11] Bennion J C, Chowdhury N, Kampf J W, et al. Hydrogen peroxide solvates of 2,4,6,8,10,12-hexanitro-2,4,6,8,10,12-hexaazaisowurtzitane[J]. *Angewandte Chemie International Edition*, 2016, 55(42): 13118−13121.

[12] Xu J, Zheng S, Huang S, et al. Host-guest nergetic materials constructed by incorporating oxidizing gas molecules into an organic lattice cavity toward achieving highly-energetic and low-sensitivity performance[J]. *Chemical Communications*, 2019, 55(7): 909−912.

[13] Saint M S, Marre S, Guionneau P, et al. Host-guest inclusion compound from nitramine crystals exposed to condensed carbon dioxide[J]. *Chemistry-A European Journal*, 2010, 16(45): 13473−13478.

[14] Cooper M S, Heaney H, Newbold A J, et al. Oxidation reactions using urea-hydrogen peroxide: a safe alternative to anhydrous hydrogen peroxide[J]. *Synlett*, 1990, 1990(9): 533−535.

[15] Liu Y, Li S, Wang Z, et al. Thermally induced polymorphic transformation of hexanitrohexaazaisowurtzitane (HNIW) investigated by in-situ X-ray powder diffraction[J]. *Central European Journal of Energetic Materials*, 2016, 13(4): 1023−1037.

[16] Turcotte R, Vachon M, Kwok Q S M, et al. Thermal study of HNIW (CL-20)[J]. *Thermochimica Acta*, 2005, 433(2): 105−115.

[17] Pu L, Xu J, Liu X, et al. Investigation on the thermal expansion of four polymorphs of crystalline CL-20[J]. *Journal of Energetic Materials*, 2016, 34(2): 205−215.

[18] Pan B, Dang L, Wang Z, et al. Preparation, crystal structure and solution-mediated phase transformation of a novel solid-state form of CL-20[J]. *Cryst Eng Comm*, 2018, 20(11): 1553−1563.

[19] Patel G N, Duesler E N, Curtin D Y, et al. Solid state phase transformation of a diacetylene by solvation. Crystal structure of a moderately reactive monomer form[J]. *Journal of the American Chemical Society*, 1980, 102(2): 461−466.

[20] Stokes S P, Seaton C C, Eccles K S, et al. Insight into the mechanism of formation of channel hydrates *via* templating[J]. *Crystal Growth & Design*, 2014, 14(3): 1158−1166.

晶胞内嵌H_2O_2分子的CL-20基主客体炸药的温和制备

余治慧[1],徐金江[2],孙善虎[2],王洪范[1],张浩斌[2],段晓畅[2],朱春华[2],王树民[1],孙 杰[2]
(1.西南科技大学材料科学与工程学院,四川 绵阳 621010; 2.中国工程物理研究院化工材料研究所, 四川 绵阳 621999)

摘 要: 六硝基六氮杂异伍兹烷(CL-20)是目前能量最高的单质炸药,为了进一步提高其爆轰性能,以过氧化脲作为H_2O_2的原料,在低温低压干燥的环境下,采用溶剂挥发法构筑了CL-20/H_2O_2主客体含能炸药。利用粉末X-射线衍射(PXRD)和拉曼光谱对其结构进表征。结果表明,制备的CL-20/H_2O_2主客体炸药是正交晶系的晶体,空间群为P_{bca},具有长程有序堆积的结构。经同步热分析仪(TG-DSC)测试得到主体CL-20分子与客体H_2O_2分子之间的摩尔比为2:1。利用原位高温XRD研究了CL-20/H_2O_2的热晶变行为,结果表明,随着温度的升高,CL-20/H_2O_2逐渐转变为γ-CL-20,并且相转变效率高于ε-CL-20。通过对CL-20/H_2O_2生长过程的追踪,观察到在溶液结晶过程中,CL-20/CH_3CN亚稳相为重要的中间体,并经过一个固相转晶过程最终形成CL-20/H_2O_2主客体炸药晶体。

关键词: 主客体炸药;六硝基六氮杂异伍兹烷(CL-20);H_2O_2;亚稳相;固相转晶
中图分类号: TJ55;O62 **文献标志码:** A **DOI:**10.11943/CJEM2019064
(责编:张 琪)